frontiers
in Marine Science

ORIGINAL RESEARCH
published: 05 October 2021
doi: 10.3389/fmars.2021.720712

River Streamflow, Remotely Sensed Water Quality, and Benthic Composition of Previously Undescribed Nearshore Coral Reefs in Northern Puerto Rico

Juan L. Torres-Pérez[1]*, Carlos E. Ramos-Scharrón[2], William J. Hernández[3], Roy A. Armstrong[4], Maritza Barreto-Orta[5], Jorge Ortiz-Zayas[6], Liane S. Guild[1] and Roberto Viqueira[7]

[1] Biospheric Science Branch, Earth Science Division, NASA Ames Research Center, Mountain View, CA, United States, [2] Department of Geography and the Environment, LLILAS-Benson, The University of Texas at Austin, Austin, TX, United States, [3] NOAA-EPP/Center for Earth System Sciences and Remote Sensing Technologies, The City College of New York, The City University of New York, New York, NY, United States, [4] NOAA CESSRST, Bio-Optical Oceanography Laboratory, Department of Marine Sciences, University of Puerto Rico, Mayagüez Campus, Mayagüez, PR, United States, [5] Graduate School of Planning, University of Puerto Rico, Río Piedras Campus, San Juan, PR, United States, [6] Department of Environmental Sciences, University of Puerto Rico, Río Piedras Campus, San Juan, PR, United States, [7] Protectores de Cuencas Inc., Yauco, PR, United States

OPEN ACCESS

Edited by:
José D. Carriquiry,
Universidad Autónoma de Baja
California, Ensenada, Mexico

Reviewed by:
Guillermo Horta-Puga,
Universidad Nacional Autónoma
de México, Mexico
Fabian Alejandro
Rodriguez-Zaragoza,
University of Guadalajara, Mexico

***Correspondence:**
Juan L. Torres-Pérez
juan.l.torresperez@nasa.gov

Specialty section:
This article was submitted to
Coral Reef Research,
a section of the journal
Frontiers in Marine Science

Received: 04 June 2021
Accepted: 15 September 2021
Published: 05 October 2021

Citation:
Torres-Pérez JL,
Ramos-Scharrón CE, Hernández WJ,
Armstrong RA, Barreto-Orta M,
Ortiz-Zayas J, Guild LS and Viqueira R
(2021) River Streamflow, Remotely
Sensed Water Quality, and Benthic
Composition of Previously
Undescribed Nearshore Coral Reefs
in Northern Puerto Rico.
Front. Mar. Sci. 8:720712.
doi: 10.3389/fmars.2021.720712

Land-based sediment stress represents a threat to many coral reefs in Puerto Rico primarily as a result of unrestricted land cover/land use changes and poor best management practices. The effects of such stresses have been documented along most coasts around the island. However, little attention has been paid to reefs located on the north coast, and very little is known about their composition and current state. Here, we present a study characterizing riverine inputs, water quality conditions, and benthic composition of two previously undescribed coral reefs (Tómbolo and Machuca reefs) located just eastward of the Río Grande de Manatí outlet in north-central Puerto Rico. This study utilizes a time series of remotely sensed ocean color products [diffuse vertical attenuation coefficient at 490 nm (Kd_{490}) and chlorophyll-a concentration (Chl-a) estimated with data from the Visible Infrared Imaging Radiometer Suite (VIIRS)] to characterize water quality in this coastal region. In general, the months with relatively high mean daily river streamflow also coincide with months having the highest proportion of eastward wave direction, which can promote the eastward influence of river waters toward the two coral reefs sites. Kd_{490} and Chl-a showed a higher riverine influence closer to the watershed outlet. Kd_{490} and Chl-a monthly peaks also coincide with river streamflow highs, particularly at those pixels closer to shore. Tómbolo Reef, located farther eastward of the river outlet, shows a well-developed primary reef framework mainly composed of threatened reef-building species (*Acropora palmata*, *Pseudodiploria*) and high coral cover (19–51%). The benthos of Machuca Reef, located closer to the river outlet, is dominated by macroalgae with a significantly lower coral cover (0.2–2.7%) mainly composed of "weedy" coral species (*Porites astreoides* and

Siderastrea radians). Cover of major benthic components correlates with distance from the river outlet, and with gradients in Kd_{490} and Chl-a, with higher coral cover and lower macroalgal cover farther from the river outlet. Coral cover at Tómbolo Reef is higher than what has been reported for similar sites around Puerto Rico and other Caribbean islands showing its ecological importance, and as up until now, an unrecognized potential refuge of reef-building threatened coral species.

Keywords: benthic cover, sedimentation, light attenuation, chlorophyll-a, macroalgae, turbidity

INTRODUCTION

While the world's coral reefs are affected by a variety of stressors, land-based sources of pollution still represent a key threat (Kroon et al., 2016; Norström et al., 2016). Therefore, a better understanding of "ridge-to-reef" connectivity is urgently needed to improve the survival of coral reefs in the Anthropocene (Hughes et al., 2017; Carlson et al., 2019). Terrigenous sediments (either suspended or bottom-deposited) are recognized as inhibitors of coral growth and detrimental to reef communities (Veron, 1995; Birkeland, 1997; McLaughlin et al., 2003). Sediments that remain suspended in the water column can affect corals by increasing turbidity and reducing the amount of photosynthetically active radiation (PAR) reaching corals (Cardona-Maldonado, 2008; Storlazzi et al., 2015). Sediments that settle on the benthos can hinder coral recruitment (Wakwella et al., 2020) or smother entire colonies (Rogers, 1990; Fabricius and Wolanski, 2000; Fabricius, 2005; Tuttle et al., 2020). Increased exposure to terrestrial sediments can reduce coral growth rates (Acevedo and Morelock, 1989; Torres, 2001; Torres and Morelock, 2002), increase coral mortality (Fabricius, 2005), and increase susceptibility to disease (Harvell et al., 2007; Cróquer and Weil, 2009). Global assessments using Geographic Information Systems (GIS; McLaughlin et al., 2003) and remote sensing show that coastal raster grid cells with high riverine runoff are much less likely to contain reefs than those away from river influence. While this might be the case at large basin-wide scales (e.g., Indo-Pacific), it might not necessarily apply at the scale of small tropical islands due to the high heterogeneity in coastal water quality (Golbuu et al., 2008; Carlson et al., 2019).

Caribbean coral reefs are no exception to the globally recognized trends (Cramer et al., 2020), and these include those within the Puerto Rico Archipelago, where coastal and marine ecosystems have long been exposed to a variety of local and regional stressors (Zuluaga-Montero, 2003; García-Sais et al., 2008; Hernández-Delgado et al., 2008; Otaño-Cruz et al., 2019). Among local impacts in Puerto Rico (PR), the effects of human land use on the exposure of coral reefs to terrestrial sediments and other pollutants ranks as the most prominent and one of the most concerning threats (Bush et al., 1995; Barreto, 1997; Morelock et al., 2000, 2010; Morelock and Barreto, 2003; Ryan et al., 2008; Hernández Delgado et al., 2017). Throughout history, land use changes in PR have represented an expression of economic development programs and population pressures (Grau et al., 2003; Rudel et al., 2010; Ramos-Scharrón et al., 2015). There is widespread consensus that the types of land use changes that occurred during the 20th and 21st century have affected soil erosion and watershed sediment delivery (Clark and Wilcock, 2000; Larsen and Santiago Román, 2001), and therefore, have altered sediment loading rates to PR's coral reef systems (Ramos-Scharrón et al., 2015; Otaño-Cruz et al., 2017, 2019). Significant land cover change in PR has included urban expansion (Pinto et al., 2009; Gellis, 2012), agricultural activities (López et al., 1998; Ramos-Scharrón and Thomaz, 2016; Ramos-Scharrón and Figueroa-Sánchez, 2017), and deforestation/reforestation (Helmer et al., 2008; Ramos-Scharrón et al., 2015). These activities also induce changes in nutrient loading and microbial pollution from inadequately treated sewage (Hernández-Delgado et al., 2008; Bonkosky et al., 2009).

Coastal water quality and climate-related factors are of great concern to local coral reef managers and stakeholders (Ballantine et al., 2008). Of particular importance is to understand the effects of anthropogenic activities within watersheds on sediment stress and nutrient discharge on coral reefs (Commonwealth of Puerto Rico and NOAA, 2010). This in turn, affects water transparency, which is a key factor for the resilience of the symbiotic relationship between reef-building coral polyps and dinoflagellates (commonly known as zooxanthellae) responsible for depositing calcium carbonate, the coral reef primary framework (Philipp and Fabricius, 2003; Putnam et al., 2017). Some of the pioneering work in the Caribbean correlating river-influenced sedimentation and reefs degradation was conducted in PR in the late 1970–1990s (Goenaga and Cintrón, 1979; Acevedo and Morelock, 1989; Rogers, 1990, among others). Similar studies (Torres, 2001; Torres and Morelock, 2002) have shown a significant reduction in linear extension rates and benthic cover of major reef-building massive species (e.g., *Orbicella faveolata*) in reefs located near river outlets when compared to those not directly influenced by riverine sediment influx. A study by Cardona-Maldonado (2008) found a significant inverse relationship between Scleractinian coral cover and PAR attenuation in 17 reefs of the west and south coasts of Puerto Rico.

Compared to other coastlines around mainland PR, the north coast presents a relatively narrow insular platform (~1.6 km in width) with moderate to high wave action from the northeast prevailing throughout most of the year. This differs from the other of the island's coastlines which in general have a much wider platform and more limited wave action (Morelock et al., 1985; Barreto-Orta et al., 2019). As such, most reef studies have concentrated in the eastern, western and southern coasts (Goenaga and Cintrón, 1979; Acevedo and Morelock, 1989; Rogers, 1990; Torres and Morelock, 2002; Cardona-Maldonado, 2008; García-Sais et al., 2008; Hernández-Delgado et al., 2008; Norat-Ramírez et al., 2019;

Otaño-Cruz et al., 2019). Nonetheless, the northern coastline features diverse natural resources including mangrove forests, beaches, rocky shorelines, nearshore coral reefs, some seagrass meadows, and salt marshes (Barreto-Orta et al., 2019). It is therefore imperative to assess the present condition of PR's coral reefs and their degree of connectivity with upland sources of sediment and pollutants, particularly at relatively unknown and understudied sites, in order to create public awareness, policies and management strategies to preserve these ecologically and economically important marine ecosystems that have lacked recognition in island-wide inventories and management plans. This includes several nearshore shallow reefs on the north coast, some of which have significant populations of threatened coral species among other important benthic components. An example of such types of reefs are those located just east of the Río Grande de Manatí (RGM) outlet into the Atlantic Ocean (**Figure 1A**). To the best of our knowledge, no previous study has assessed the biotic structure and status of such reefs and the potential influence of the RGM sediment plume.

This study aims to: (1) describe the hydrologic and ocean wave controls on coastal water quality conditions along an east-west virtual transect near the vicinity of the RGM outlet; and (2) characterize two previously undescribed coral reef sites located just east of the RGM outlet in terms of cover, species composition, and water quality.

MATERIALS AND METHODS

Study Sites

The Manatí shoreline is dominated by sandy beaches, the outlet of the RGM, eolianites (lithified dunes), and exposed beach rock formations that extend from the shoreline to open waters. The benthic assessment component of this study was conducted at two sites in close proximity to the RGM watershed outlet in northcentral Puerto Rico, namely the Tómbolo (18°28.981N; 66°31.396W) and Machuca Reefs (18°29.053N; 66°31.643W) (**Figures 1A,B**). Land access to both Tómbolo and Machuca beaches is limited and controlled as these are managed for cultural and natural resource conservation purposes as Hacienda Esperanza by the non-profit organization known as Para La Naturaleza.

Tómbolo Reef has an approximate area of 73,200 m^2 and is located contiguous to Tómbolo Beach with a substrate dominated by a combined eolianite and beach rock formation colonized by hard (Scleractinian) and soft (mostly sea fans, gorgonians) corals, with intermingled pavement and sandy patches. The site reaches

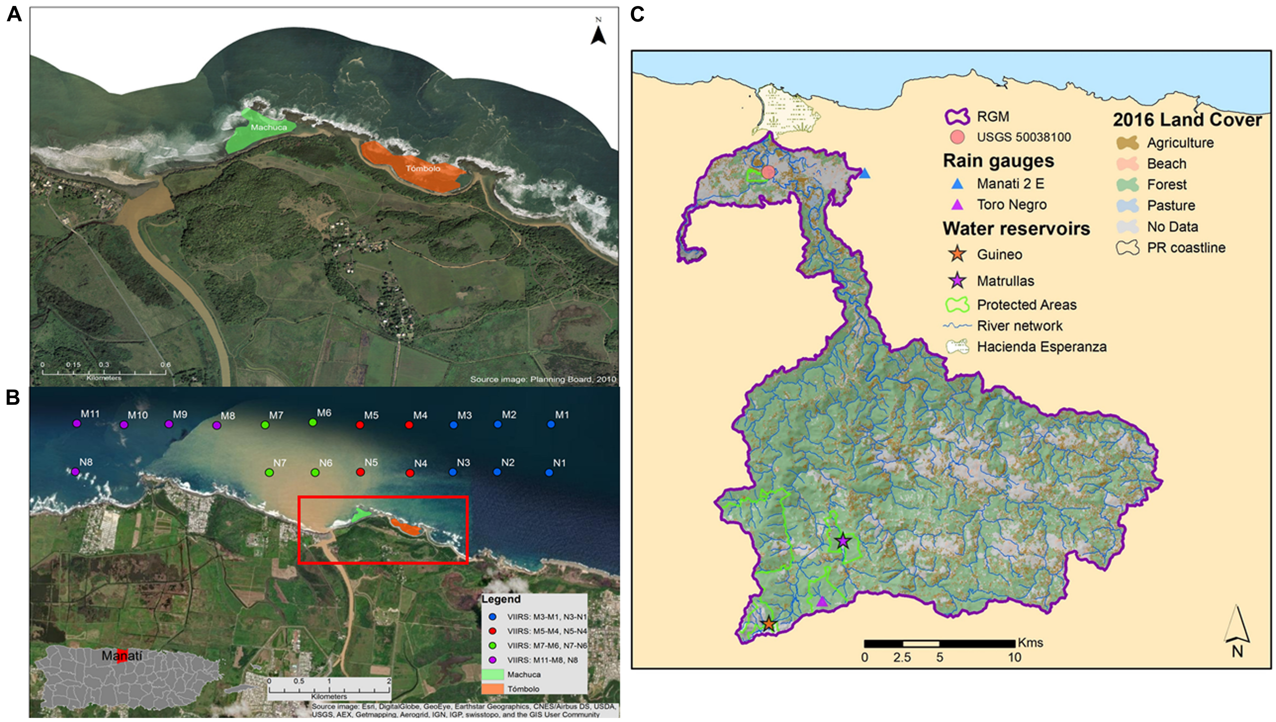

FIGURE 1 | (A) Worldview image (provided by the PR Planning Board) showing the location of the Machuca and Tómbolo Reefs (green and orange polygons, respectively) in reference to the RGM outlet in north coast, Puerto Rico. **(B)** Worldview image from a November 2014 rainfall event showing the extent of the river plume. The centers for each VIIRS virtual station (750 m pixel size) (N1–N8: nearshore; M1–M11: mid-platform) are superimposed. A map of Puerto Rico showing the location of the municipality of Manatí on the north coast is included for reference. An oceanic station (O1; not shown here) located approximately 25 Km north of the study sites was used as a reference for oligotrophic waters (Case 1) (see section "Satellite-Based Water Quality Parameters"). **(C)** 2016 RGM watershed map with major land cover classes. Only two reservoirs (Guineo and Matrullas) are located within the watershed boundaries. The Hacienda La Esperanza Reserve on the northern part of the watershed is also shown as well as the location of the USGS streamflow station (50038100).

the water line at the beach and extends seaward to a beach rock formation that forms a barrier and separates it from the open ocean. Depth ranges from 0 m near the beach waterline to less than 3 m at its deepest zone about midway between the beach and the beach rock formation. The shallowest zones on the westward side are dominated by elkhorn coral (*Acropora palmata*), the hydrozoan *Millepora* sp., and the zoanthid *Palythoa caribaeorum*. Brain corals (*Pseudodiploria strigosa* and *Pseudodiploria clivosa*) dominate the benthic sessile fauna on the eastward side.

Machuca Reef has an approximate area of 44,600 m^2 and is located contiguous to Machuca Beach. This is a very shallow site with depths ranging from 0 to 2 m. The substrate has an eolianite composition covered by dead hard coral colonies colonized by either turf or macroalgae (*Dictyota* sp.) and very limited live coral cover, mostly considered to be sediment-resistant species like *Siderastrea siderea*, toward the westward side and a sandy layer dominated by turtle grass, *Thalassia testudinum*. Additionally, the westward side of Machuca Reef opens directly eastward toward the RGM outlet. A beach rock barrier separates this site from the Tómbolo site impeding the exchange of water between them.

Marine ecosystems in the Tómbolo and Machuca areas have been presumed to be impacted by land use patterns occurring within the watershed which have likely led to increased exposure to terrestrial sediments, nutrients, and other pollutants. Initial visual inspections conducted by our team in 2010 showed marked differences in coral cover between sites. No previous study has assessed the biotic structure of both reefs associated with this watershed despite being one of the few coral reef frameworks in the north coast of Puerto Rico. In fact, coral reefs are not included as part of the natural resources found within the Hacienda La Esperanza description (Wusinich-Méndez et al., 2007) and similar publications describing reef formations in northern Puerto Rico (Ballantine et al., 2008).

Historical Land Use and Hydrological Background of the Río Grande de Manatí Watershed

The RGM is located in central PR and is one of the large watershed areas draining toward the north coast of the island (**Figure 1C**). RGM extends inland for about 35 km and has an approximate area of 449 km^2. RGM has three main physiographic areas including portions of the central upland province of the Cordillera Central, a slice of the northern karst province, and parts of the alluvial northern coastal plains (Monroe, 1980). Annual rainfall averages from 1,570 mm yr^{-1} in the lowland alluvial valley (Manatí 2 E Station: MAN, RQC00665807) to 2,360 mm yr^{-1} at its highest elevations [$\sim$1,210 m above sea level (a.s.l.)]. Monthly rainfall follows the bimodal pattern typical of the Insular Caribbean (Ángeles et al., 2010) with approximately 17–22% of the annual total occurring during the months of April–May and about 50% from August to November (Daly et al., 2003). The RGM has one of the highest discharges of the island ($\sim$10.7 m^3 sec^{-1} or 92.5 × 10^4 m^3 day^{-1}; Larsen and Webb, 2009). Dominant land use within the watershed includes agriculture (e.g., coffee and plantains), cattle farms, recreational activities involving the upper parts of the river (e.g., off-road vehicle tracks), and others that contribute to the river sediment load. However, landslides have been found to be an important source of the sediment budget of watersheds throughout PR (Larsen, 2012; Ramos-Scharrón et al., 2021) and RGM is likely not an exception.

Río Grande de Manatí Rainfall and Streamflow Data Analyses

We relied on rainfall data collected at two distinct elevations to describe both long-term and study period rainfall patterns in RGM. The two rainfall stations analyzed were the Manatí 2 E station (MAN; RQC00665807) located at the alluvial valley of the RGM at an elevation of 76 m a.s.l., and the Toro Negro Forest station (TNF; RQC00669432) near the western ridgeline of the watershed at 868 m a.s.l. (data downloaded from https://www.ncdc.noaa.gov/cdo-web/). Rainfall during the 2012–2019 study period was compared against long-term monthly averages and variance (i.e., normal and both 25 and 75% quartiles) to evaluate the representativeness of the study period relative to long-term conditions and to identify any anomalous dry and wet periods. Rainfall results are included as **Supplementary Figure 1**.

Streamflow collected at the lowermost United States Geological Survey gauging station in the RGM watershed (USGS 50038100; Lat: 18°25′51.858N; Long: 66°31′36.612W; 4.3 m in elevation, 414.3 km^2) was used as representative of the discharge reaching the watershed outlet (data downloaded from https://waterdata.usgs.gov/nwis). Data for the study period only included the months of January-2012 to May-2019 due to an equipment failure in June-2019. The study period streamflow was compared against the entire preceding period of record (January-1970 to December-2011) through ANOVA analyses of log-transformed daily average flows (in units of m^3 day^{-1}) over the entire dataset and for each individual month of the year. This was done to establish if the study period was representative of long-term conditions, to describe its temporal variability, and any deviations from normality. A one-way ANOVA and Tukey-Honest Significant Difference (HSD) test were used for datasets with equal variance and one-way Kruskal–Wallis non-parametric ANOVA and Dunn's test for months with unequal variance determined using a Levene's test. Most of these data are included as **Supplementary Figure 2**.

Historical Wave Regime

Ocean wave approach angle can exert an influence on the direction and extent of riverine sediment plumes. To describe the wave regime on the north coast of PR, wave direction data (in degrees) were obtained from the Caribbean Coastal Ocean Observing System (CariCOOS)[1] for the San Juan Buoy (41053) for 2012–2019. Data summaries are included as **Supplementary Figure 3**. These data were used to: (1) establish which months have a higher chance of eastward currents; and (2) analyze if months with higher river discharge also coincide with those with a higher chance of eastward currents.

---

[1] https://www.caricoos.org/data-download

Satellite-Based Water Quality Parameters

The prevailing strong wind and wave action along this coastline throughout most of the year makes the regular collection of *in situ* data practically impossible and highly dangerous for field personnel. Instead, we used the NASA-NOAA's Suomi National Polar-orbiting Partnership (NPP) Visible Infrared Imaging Radiometer Suite's (VIIRS) diffuse vertical attenuation coefficient at 490 nm (Kd_{490}) (Wang et al., 2009) and chlorophyll-a (Chl-a; Wang and Son, 2016) daily products tailored for PR as an approximation for evaluating patterns of water quality near the shoreline (Hernández et al., 2020). A total of 2,921 VIIRS daily images from January 2012 to December 2019 were obtained through the NOAA Coast Watch website[2] at Level 2 Science Quality accessed in March 2020 and a time-series was develop for the study area. Kd_{490} and Chl-a values were compiled for locations just offshore from the RGM outlet, but only 708 images of the potential 2,921 provided useful data. The limited number of useful images were mainly due to clouds as these frequently obscured portions of the area of interest (Mikelsons and Wang, 2019).

Two parallel transects, one nearshore and one immediately north, including a total of nineteen (19) VIIRS 750 m pixels ("virtual stations") just north of the reef sites were chosen (**Figure 1B**). Values were compiled daily, monthly and seasonally for 2012–2019. Due to the limited number of cloudless images available, we chose to use the entire dataset available to have a better understanding on the seasonal variation in Kd_{490} and Chl-a at distinct distances from shore. VIIRS has a relatively coarse spatial resolution (750 m) which limits the use of its data at the shoreline as mixed land/water pixels may occur. Therefore, care was taken into choosing pixels not influenced by shoreline features. As such, the virtual stations were located eastward, northward and westward of our study sites. An oceanic pixel was also included at approximately 25 km north of the study area to provide a reference oceanic value for both Kd_{490} and Chl-a. The Kd_{490} and Chl-a monthly means (2012–2019) for each virtual station were log-transformed and analyzed with a one-way ANOVA. For *post hoc* or multiple comparisons, a Tukey's Honest Significant Difference Contrasts method (Tukey's HSD) was applied to test for differences among the virtual stations. A two-way ANOVA was used to test for spatial and temporal differences in Kd_{490} and Chl-a during months of high river streamflow for virtual stations located just north of the river outlet (N6, N7), near Machuca Reef (N5), and near Tómbolo Reef (N4) using the months and virtual stations as the two factors evaluated.

In-Water Benthic Sampling for Reef Characterization

A series of 30 m "square transects" were established in both study sites (Tómbolo Reef, $n = 8$; Machuca Reef, $n = 4$) in 2015–2016. Briefly, a main 10 m metric tape was established, and two additional 10 m lines were located perpendicular at the 3 and 7 m marks (see **Supplementary Figure 4** for a drawing of the sampling design). At each transect, 30 intercalated 1 m^2 polyvinyl chloride (PVC) quadrats were laid. Each quadrat was further sub-divided into four 0.5 m × 0.5 m sub-quadrats. Photos were taken perpendicular to each sub-quadrat to allow for a more precise benthic classification. A total of 120 (0.5 m× 0.5 m) photos (four photos per 1 m^2) per each 30 m transect were used in the analysis. We opted for this atypical design as it allows for the assessment of a wider surface area than standard line or belt transects. The total number of "square transects" was different among study sites due to the limited amount of time divers were able to stay and safely maneuver in the water. Wave action along this coastline is usually high and the window for field work is limited to a few hours early in the morning and only during several days of the year, particularly at the Machuca site which is more exposed than Tómbolo. Sampling depth was kept constant at both sites (<2 m). Additionally, macro photos of rare or small benthic components (where appropriate) were taken to help identify specific specimens.

Photoquadrat Analysis

Photoquadrats from each transect were analyzed using the "Coral Point Count with Excel extensions" (CPCe) package (Kohler and Gill, 2006). CPCe corrects/georectifies the photographic image and establishes unbiased random distribution of a number of points onto an underwater photographic image to enable the visual identification of each feature lying under each point (Kohler and Gill, 2006) for statistical analyses of species per substrate. The result is an unbiased estimate of benthic composition. As such, 25 random points were generated for each 0.5 m× 0.5 m photoquadrat for a total of 3,000 random points analyzed per each 30 m transect. The identification of benthic organisms was performed visually to the lowest taxonomical level possible usually to the genus or species level in the case of living substrates (some components like turf algae were only identified as such). Photos of common species collected by the main author over 30 years of diving in Puerto Rican waters as well as additional macro photos taken during the field campaign were used as reference when in doubt. Coral reef ID literature (e.g., Colin, 1978; Littler and Littler, 2000; Humann and DeLoach, 2013; Veron et al., 2016) was also used as reference. Presence or absence of health parameters such as bleaching or diseases in reef corals was also noted. CPCe uses a hierarchical categories system with major categories sub-divided into more specific ones, where appropriate. For the purpose of this analysis, the major categories included Scleractinian Corals (C), Seagrasses (GRASS), Octocorals (G), Macroalgae (MA), Sponges (S), Zoanthids (Z), Coralline Algae (CA), and a single category including Sand, Pavement, and Rubble (SPR). Here, MA includes green, brown and red macroalgal forms as well as turf algae. All coralline algae (CA) at both sites were encrusting forms and no geniculate forms were found.

Statistical Analysis of Benthic Composition

The percent cover of each taxon or substrate type was obtained with the automatic generation of analysis spreadsheets of the CPCe software. CPCe calculates percent cover of each benthic

---

[2] https://coastwatch.noaa.gov/

substrate type based on the number of points intercepting each species, divided by the total of points in the quadrat (Kohler and Gill, 2006). Afterward, these data were arcsine transformed prior to the statistical analysis (Ott, 1993). The data was analyzed based on one factor (Reef) and two levels (Tómbolo vs. Machuca) with transects as replicas. As such, a Student's *t*-test was applied to test for differences in benthic composition among reef sites. A square-root transformation was performed followed by a Bray-Curtis indices to quantify the compositional dissimilarity between the two study sites followed with a non-metric Multidimensional Scaling (nMDS) approach. Finally, a Principal Components Analysis (PCA) was computed to identify which coral species contributed the most variation in coral species cover among sites. Overall percent cover of the major categories was further correlated with distance from the river outlet obtained with satellite imagery using a Pearson's Correlation Matrix.

Diversity indices were generated by CPCe and incorporated in the analysis. CPCe automatically calculates a Shannon-Weaver and a Simpson's Diversity Indexes based on the major categories for each site. We applied a Student's *t*-test to test for differences in these two indices in both sites (Ott, 1993). All univariate statistical analyses were performed with OriginPro2019®. Multivariate analyses (nMDS and PCA) were performed with PRIMER® v6.0.

RESULTS

Río Grande de Manatí Rainfall and Streamflow

The 2012 to 2019 study period is representative of long-term rainfall for RGM and that includes not only normal seasonal amounts and variability but also both severe drought conditions and extreme rainfall maxima. Rainfall followed the expected seasonal patterns with relative highs in April–May and September–November but it was highly variable (see **Supplementary Figure 1**). Mean daily flow from 1970 to 2011 was 111 $m^3 \times 10^4\ d^{-1}$ and this translates to an area-normalized equivalent of 980 $mm\ y^{-1}$ (assuming a contributing area of 413.4 km^2) that is within the range of values reported for large watersheds draining wet regions in PR (Larsen and Webb, 2009). Individual daily values from 1970 to 2011 ranged from 7.6 to 19,670 $m^3 \times 10^4\ d^{-1}$ on 24-January-95 and 22-September-98 (Hurricane Georges), respectively. Monthly streamflow is highly seasonal with a bimodal distribution (**Supplementary Figure 2A**). The month of May represents an early peak followed by September, October, and November. Each of these 4 months is responsible for ~14% of the annual runoff. Monthly streamflow during these 4 months is statistically different than the drier months of January through March and June to July (see **Supplementary Figure 2**). The months of April, August, and December normally represent transitional periods between dry and wet months.

Considering all daily streamflow data collected for 1970–2011 and 2012–2019, streamflow during the two periods was statistically undistinguishable (**Supplementary Figure 2B**). Mean streamflow for 2012–2019 was only slightly lower at 105 $m^3 \times 10^4\ d^{-1}$ (925 $mm\ y^{-1}$) with values ranging from 6.0 to 14,800 $m^3 \times 10^4\ d^{-1}$ [21-April-2019 and 20-September-2017 (Hurricane María), respectively]. However, out of a total of 89 months with streamflow data, 64 months or 72% had monthly streamflow values that were below normal. Only 25 months out of 89 (28%) had flows that exceeded normal monthly averages. This pattern of low streamflow relative to normal interrupted by sporadic extreme events is exactly the type of effect projected to become more prominent in the Caribbean as a consequence of global climate change (Reyer et al., 2017).

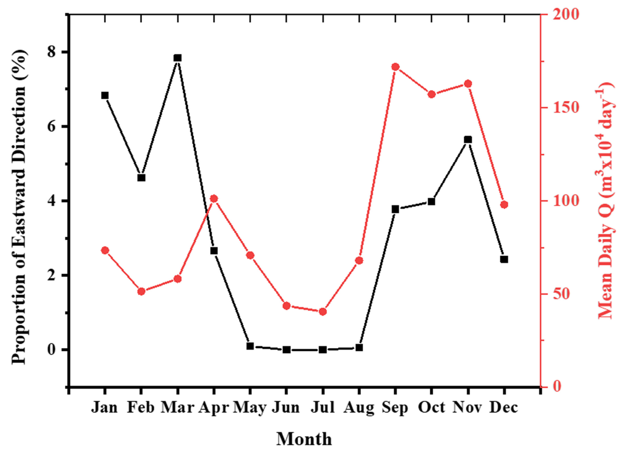

FIGURE 2 | Comparison of longshore currents direction on the north coast as measured by the San Juan buoy vs. mean RGM streamflow for 2012–2019. Red dots and black squares represent the mean daily Q and mean proportion of eastward longshore current direction for each month.

Wave Approach Direction (2012–2019)

Data from the San Juan buoy shows waves typically approaching from the northeast (dominant azimuth of 53°) for 2012–2019. Wave approach is predominantly westward with only a small percentage (maximum of 8% per month) of eastward trending waves occurring typically mostly between January–April and September–December. Months with the highest proportion eastward trending waves are those with highest monthly flows at RGM (**Figure 2**).

Remotely Sensed Water Quality Parameters

Both Kd_{490} and Chl-a showed a pattern of reduced values with distance from the river outlet, particularly on an eastward direction (**Figure 3**). Nearshore virtual stations (N1–N8) showed the highest range of Kd_{490} with those farther from the river outlet showing the lowest overall values (N1: 0.034–0.107 m^{-1}) and the one just north of the outlet having the highest values (0.055–1.112 m^{-1}). Kd_{490} values for those stations located just north of the study sites (N4: Tómbolo, and N5: Machuca; see **Figure 1** for reference) were similar during the driest month (July) (0.038 and 0.044 m^{-1}, respectively). Nonetheless, Kd_{490} values for N5 doubled those of N4 during the wettest months (October–November) (0.360–0.385 and 0.175–0.182 m^{-1}, respectively). A similar pattern was found for

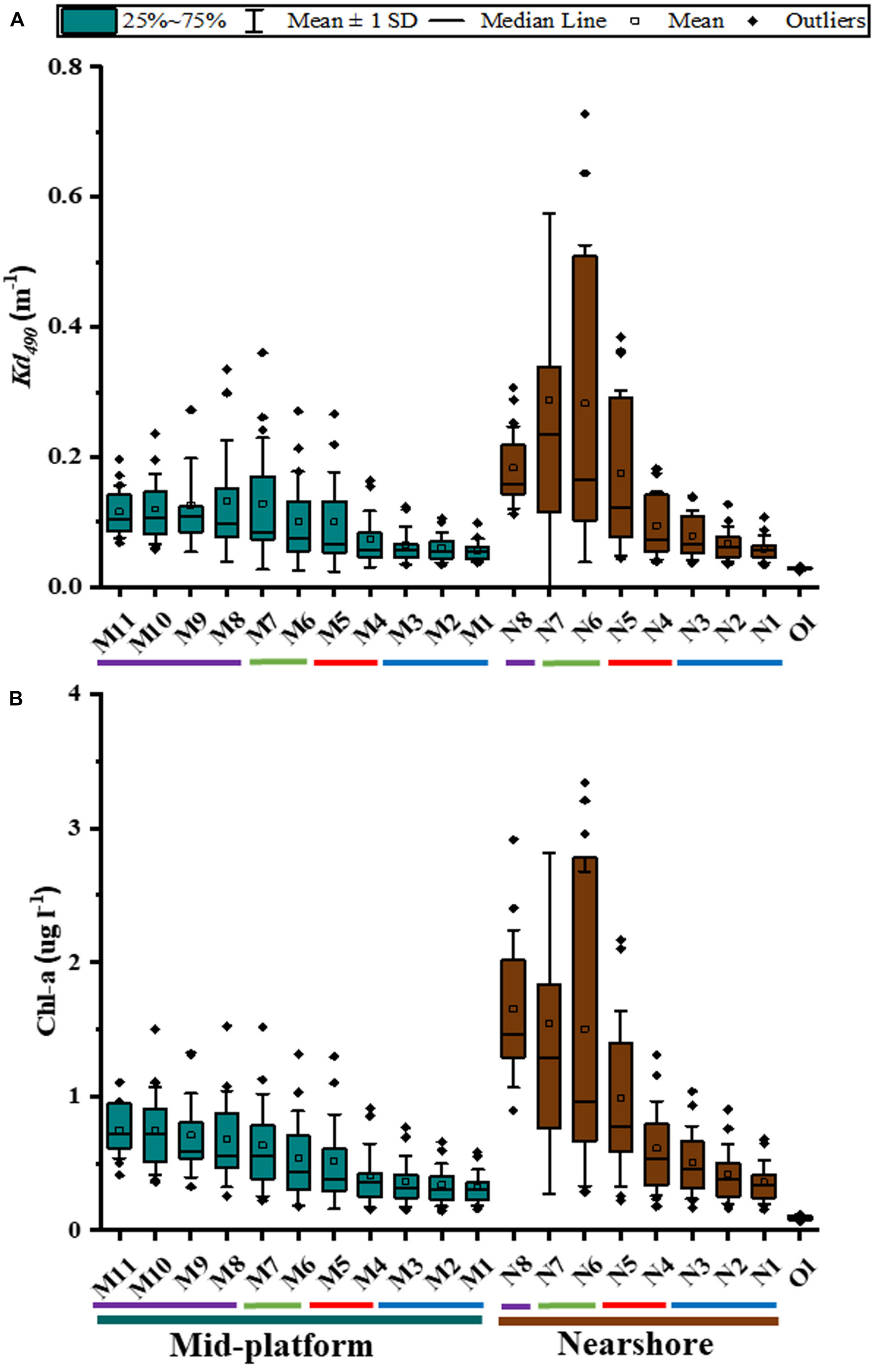

FIGURE 3 | (A) Vertical attenuation coefficient (Kd_{490}) and, **(B)** chlorophyll-a concentration estimated with VIIRS data for pixels (virtual stations) located immediately north of the study sites (January 2012–June 2019). Names for virtual stations are based on the same nomenclature used in **Figure 1**. *X*-axis: Blue bar, mid-platform virtual stations (M1–11); Brown bar, nearshore virtual stations (N1–8); O1, 25 km offshore virtual station.

Chl-a with the farther eastward station showing the lowest values (N1: 0.154–0.680 µg l^{-1}) and that just north of the river outlet showing the highest values (0.328–5.149 µg l^{-1}). Chl-a values of stations just north of the study sites were higher at N5 during any given month (0.224–2.170 µg l^{-1}) compared to N4 (0.178–1.312 µg l^{-1}). Chl-a values during the wettest months (October–November) ranged from 1.157 to 1.312 µg l^{-1} at N4 and 2.105 to 2.170 µg l^{-1} at N5. Kd_{490} and Chl-a values were constantly lower at any mid-platform virtual station (M1–M11) compared to those at their equivalent nearshore station (N1–N8). The oceanic station (O1) consistently displayed small Kd_{490} and Chl-a values

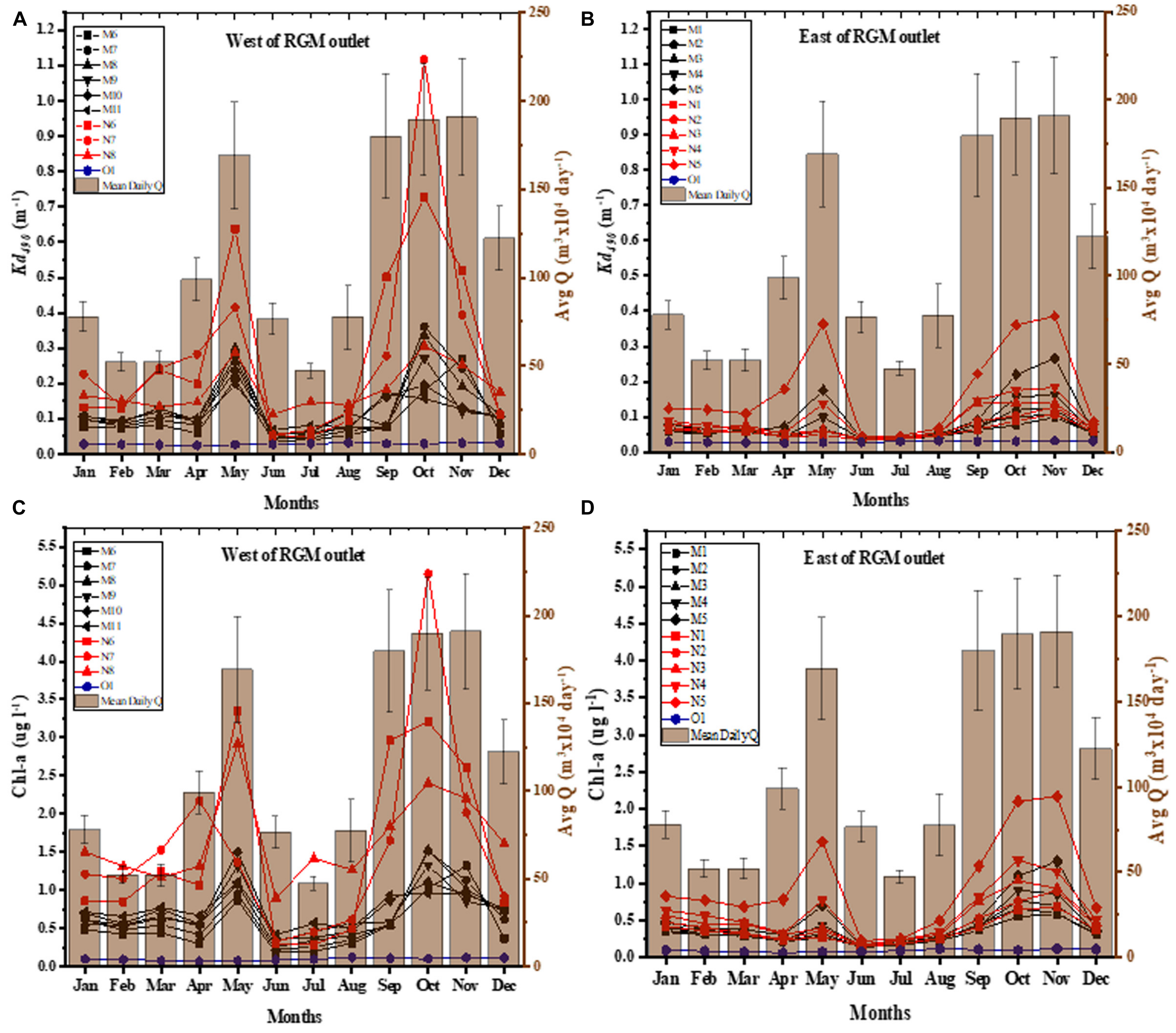

FIGURE 4 | VIIRS time-series analysis (nearshore stations) from 2012 to 2019 of Kd_{490} and Chl-a compared to monthly mean of Q (from the USGS RGM streamflow station) for each month of the year. **(A)** Kd_{490} for virtual stations north-west of the river outlet (nearshore: N6–N8; mid-platform: M6–M11). **(B)** Kd_{490} for virtual stations east of the river outlet (nearshore: N1–N5; mid-platform: M1–M5). **(C)** Chl-a for virtual stations north-west of the river outlet (nearshore: N6–N8; mid-platform: M6–M11). **(D)** Chl-a for virtual stations east of the river outlet (nearshore: N1–N5; mid-platform: M1–M5).

(0.024–0.032 m^{-1} and 0.064–0.117 µg l^{-1}, respectively) for all months-years representative of oligotrophic waters with no apparent influence of riverine discharges at that distance (∼25 km from shore).

Water quality data obtained from VIIRS were tested for normality prior to the analysis of differences among means (ANOVA) and individual means comparison (Tukey's HSD test). VIIRS data for Kd_{490} and Chl-a (**Figure 4**) showed significant differences among virtual stations (one-way ANOVA; $p < < 0.0001$ for Kd_{490} and $p < < 0.0001$ for Chl-a). When considering any given month for the 2012–2019 period, a multiple comparison analysis (Tukey's HSD test; see **Supplementary Table 1**) showed no significant differences in average Kd_{490} and Chl-a between the virtual stations located just north of the river outlet and Machuca Reef (N6–N7 and N5, respectively) suggesting an apparent influence of the river plume at Machuca all year round. Kd_{490} and Chl-a data for N4 (just north of Tómbolo Reef) were not significantly different than that of N5 when the entire dataset is considered (dry and wet months).

A Student's t-test was then applied to the Kd_{490} and Chl-a data for those virtual stations closer to the study sites (N4 and N5) for the months with higher than mean daily streamflow (January, April–May, September–December). Kd_{490} was significant lower at N4 (0.071–0.182 m^{-1}) than at N5 (0.086–0.385 m^{-1}) ($p = 0.031$) whereas Chl-a concentration differences were borderline not significant (N4: 0.329–1.312 µg l^{-1}; N5: 0.671–2.170 µg l^{-1}) ($p = 0.067$). These results suggest that light attenuation differences between both virtual stations are most likely influenced by other Case 2 water constituents like suspended solids (i.e., sediments) rather than chlorophyll-a (Doron et al., 2007; Wang et al., 2009). No

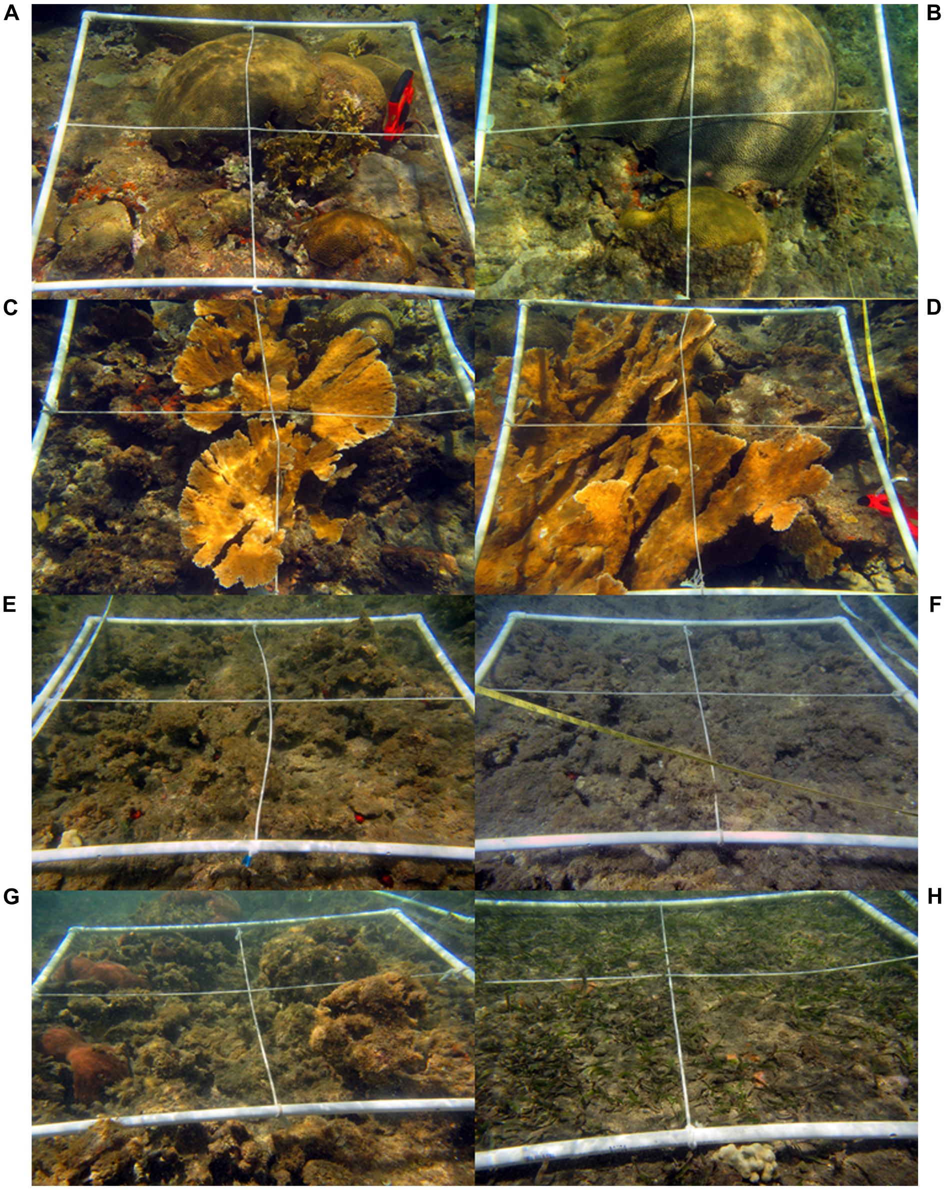

FIGURE 5 | Representative quadrats of the Tómbolo Reef **(A–D)** and Machuca Reef **(E–H)** benthos. Note the presence and dominance of reef-building Caribbean Scleractinian coral species at Tómbolo vs. the dominance of dead coral colonies covered by diverse macroalgal species and some seagrasses beds at Machuca. Some of the few live hard coral colonies (*S. siderea*) found at Machuca Reef can be seen on the lower left photo **(G)**.

total suspended solids products were available from VIIRS to compare these results. There were no significant differences found between nearshore stations located farther eastward from the river outlet (e.g., N1, N2) and those located farther away from shore toward the northeast (e.g., M1, M2) for both Kd_{490} and Chl-a suggesting there is minimal to no influence of the RGM plume at such distance and direction. No differences were found between the offshore station (O1) mid-platform (M1–M11) and nearshore east (N1–N4) stations when data from low and high river flow periods were combined. Kd_{490} and Chl-a values for O1 were significantly different than those of N5–N7 for all months combined (one-way ANOVA; $p < < 0.0001$ for Kd_{490} and $p < < 0.0001$ for Chl-a) and for those months of higher than mean streamflow (one-way ANOVA; $p < < 0.0001$ for Kd_{490} and $p < < 0.0001$ for Chl-a).

A seasonal analysis (**Figure 4**) from 2012 to 2019 of Kd_{490} and Chl-a shows two peaks during the months of April–May and again from September to November corresponding to the Spring and Fall rain seasons and relatively higher streamflow in PR for those stations near the river outlet (i.e., N6–N7) and just north of Machuca Reef (N5). These peaks coincide with the months with the highest mean daily streamflow of the RGM and with months when there is a higher proportion of eastward

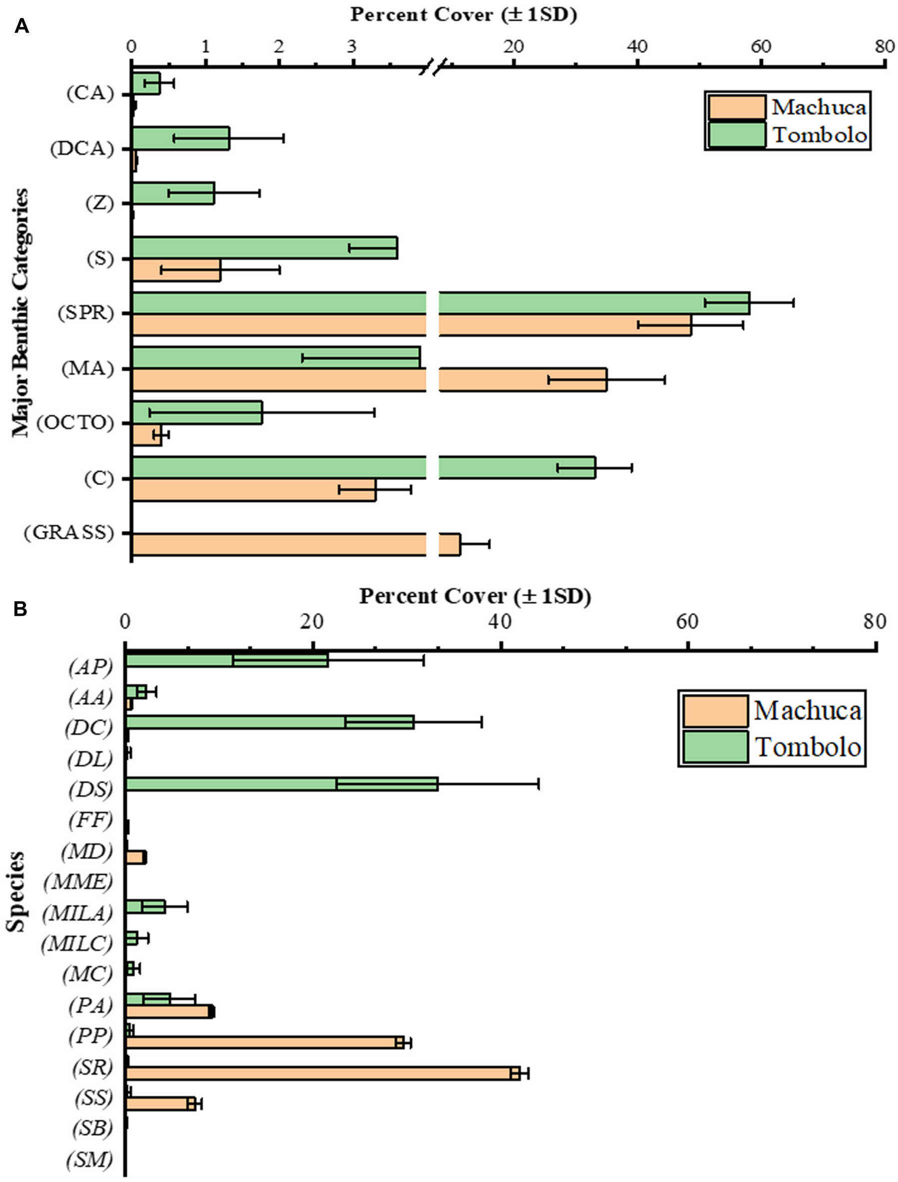

FIGURE 6 | (A) Percent cover of major categories (±1 SD) of benthic substrates at both study sites. Categories abbreviations: Scleractinian Corals (C), Macroalgae (MA), Seagrasses (GRASS), Octocorals (G), Sponges (S), Zoanthids (Z), Coralline Algae (CA), and Sand, Pavement, and Rubble (SPR). **(B)** Distribution of Scleractinian and Milleporid species (by percentage ±1 SD) at both study sites. Total Scleractinian cover at Tómbolo Reef averaged 33% (±5.96) and at Machuca Reef averaged 3.3% (±0.48). The graphs show the breakdown by species of that percentage. Species abbreviations: *Acropora palmata* (AP), *Agaricia agaricites* (AA), *Pseudodiploria clivosa* (DC), *Diploria labyrinthiformis* (DL), *Pseudodiploria strigosa* (DS), *Favia fragum* (FF), *Madracis decactis* (MD), *Meandrina meandrites* (MME), *Millepora alcicornis* (MILA), *Millepora complanata* (MILC), *Montastraea cavernosa* (MC), *Porites astreoides* (PA), *Porites porites* (PP), *Siderastrea radians* (SR), *Siderastrea siderea* (SS), *Solenastrea bournoni* (SB), and *Stephanocoenia michelini* (SM).

longshore currents (**Figure 2**). The highest average values for any given month for Kd_{490} were 1.12 m^{-1}, and Chl-a with 5.14 $\mu g\ l^{-1}$, both corresponding to N7 just north of the RGM mouth in October (averaged for 2012–2019). The highest values of Kd_{490} and Chl-a for the virtual station closer to Machuca Reef (N5) were 0.38 m^{-1} and 2.17 $\mu g\ l^{-1}$, respectively, in November (averaged for 2012–2019). These values are very similar to those at N7 for the same month (Kd_{490} = 0.39 m^{-1} and Chl-a = 2.01 $\mu g\ l^{-1}$). In contrast, the highest values of Kd_{490} and Chl-a for the virtual station closer to Tómbolo Reef (N4) were 0.182 m^{-1} and 1.312 $\mu g\ l^{-1}$, respectively, in October (averaged for 2012–2019).

Coral Community Structure and Benthic Cover

The reef community contrasts significantly at both studied sites with the Tómbolo Reef having a dominant Scleractinian-based benthos and the Machuca Reef being dominated by macroalgae

TABLE 1 | Bray-Curtis similarity analysis for all transects at both sites.

Transects	T1	T2	T3	T4	T5	T6	T7	T8	M1	M2	M3	M4
T1												
T2	72.252											
T3	57.870	76.833										
T4	68.705	85.628	81.069									
T5	71.686	92.106	78.742	84.516								
T6	54.607	44.754	33.874	42.416	44.687							
T7	43.387	69.488	73.421	64.824	70.140	39.862						
T8	68.411	70.808	59.804	67.233	69.442	73.799	63.792					
M1	21.724	13.512	15.865	13.854	17.577	3.694	8.717	9.007				
M2	20.156	15.251	10.129	11.524	20.207	4.805	11.333	5.886	53.059			
M3	20.828	15.334	11.573	13.510	20.020	4.397	10.372	5.442	61.203	73.245		
M4	30.762	26.168	23.629	24.719	30.864	11.708	16.968	15.197	56.163	55.250	75.940	

MT, Tómbolo Reef transects; MM, Machuca Reef transects.

and dead surfaces. **Figure 5** shows representative photos of photoquadrats from both sites. A complete list of all coral species (present and absent) at both sites can be found in the **Supplementary Table 2**.

The benthos and substrates at Tómbolo Reef are dominated by a mix of SPR (58.04 ± 7.21%) followed by Scleractinian corals (33.04 ± 5.96%). All other major categories accounted for less than 4% on average individually (**Figure 6A**). Macroalgal cover at Tómbolo (3.91 ± 1.6%) was mostly dominated by thin turf algae, *Dictyota* sp., and *Dictyopteris* sp.

In terms of Scleractinian species, the threatened *Acropora palmata* (79 FR §53852, 2014) as well as other important Caribbean reef-builders (*Pseudodiploria clivosa* and *P. strigosa*) dominate at Tómbolo (**Figure 6B**). Other less conspicuous but common Caribbean species (i.e., *Porites astreoides*, *Porites porites*, *Montastraea cavernosa*, and *Agaricia agaricites*) were also present in lesser amounts. Milleporids, particularly *Millepora alcicornis* and to a lesser extent *Millepora complanata*, were also an important component of the calcifying Cnidarian fauna at Tómbolo Reef.

Gorgonia ventalina dominates the octocoral fauna at Tómbolo along with the encrusting *Erythropodium caribaeorum* which tends to compete with Scleractinians for space. Nonetheless, the average cover of the latter accounts for less than 2% of the substrate. A few (less than ten) small colonies of *Plexaura* sp. were also identified at Tómbolo. Particularly in the very shallow zones (<1–2 m depth), the zoanthid *Palythoa caribaeroum* also competes for space although its cover did not account for more than 2% of the total benthic cover. Echinoids, mainly *Echinometra* sp., *Tripneustes ventricosus*, and *Diadema antillarum* were seen between small crevices in pavement zones or beneath mounding coral colonies. Individuals of the flamingo tongue, *Cyphoma gibbosum* were commonly spotted predating on *G. ventalina* colonies at Tómbolo.

The Machuca Reef substrate is characterized by flattened dead coral colonies covered by algae, mostly turf and *Dictyota* sp. in very shallow waters (<2 m depth). SPR dominates a large portion of the substrate as well (48.57 ± 8.51%) (**Figure 6A**). Scleractinian corals only accounted for 3.30 ± 0.48% of the benthos with only a few colonies of what are considered to be sediment resistant species (i.e., *Siderastrea radians, S. siderea*, *Madracis decactis*, *P. astreoides*, and *P. porites*) found within the studied transects (**Figure 6B**). Some *S. siderea* colonies were infected with red spot disease. No octocorals were found at Machuca Reef with the exception of a single small colony of *G. ventalina* in one of the transects. Similarly, only one small colony of the zoanthid *P. caribaeroum* was seen in the area. Small (less than 5 cm tall) tubular sponges were spotted in a few areas as well as some encrusting yellow-orange ones most likely from the genus *Myrmekioderma*. However, the average sponge cover at Machuca was minimal (1.2 ± 0.8%). Echinoids, particularly *Echinometra* sp., were present inside reef crevices at all transects where macroalgal cover was dominant.

Macroalgal cover at Machuca (34.96 ± 9.45% of the total benthic cover) was dominated by turf algae, the Phaeophytes *Dictyota* sp. and *Padina* sp., and the Chlorophytes *Ulva lactuca*, *Enteromorpha* sp., and *Penicillus* sp. The Rhodophyte *Liagora* sp., which is typically abundant in deeper reef zones, was present throughout the studied transects at Machuca (4.53 ± 0.35%).

Student's *t*-tests showed significant differences in the means of two of the three dominant major categories: corals ($p < < 0.0001$) and macroalgae ($p < < 0.0001$). SPR means were not significant at $\alpha = 0.05$ ($p = 0.662$). The Bray-Curtis analysis (**Table 1**) and the nMDS (**Figure 7A**) showed a distinct separation between Machuca and Tómbolo based on the distribution of major benthic categories. The first two principal components of the PCA based on the abundance of coral species accounted for 84.5% of the variation between sites with the PC1 dominated by the presence of *S. radians*, *P. porites*, *P. strigosa*, *P. clivosa*, and *A. palmata* whereas the PC2 was dominated by *A. palmata*, *P. clivosa*, and *P. strigosa* (**Figure 7B**).

Both sites showed a relatively low diversity as shown by the Shannon-Weaver (Tómbolo: 1.10 ± 0.18; Machuca: 0.72 ± 0.19) and Simpson's indexes (Tómbolo: 0.56 ± 0.07; Machuca: 0.37 ± 0.13) based on the sum for all major categories. This is also somewhat reflected in the coral community. Corals at Tómbolo included about 14 different species but were clearly dominated by

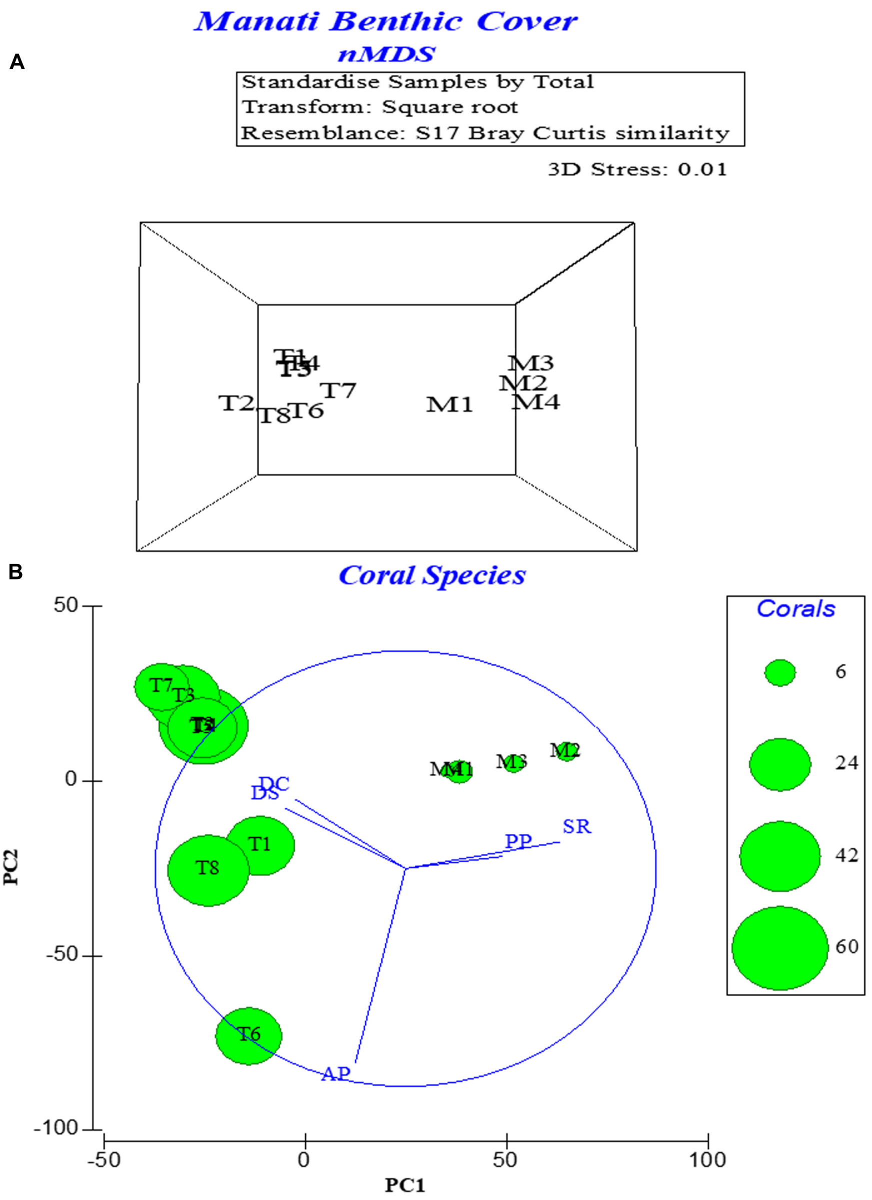

FIGURE 7 | Multivariate statistical analysis of benthic cover data. **(A)** nMDS 3-D plot showing the separation of both sites transects obtained with the Bray-Curtis resemblance matrix and based on the dominance of major categories. **(B)** PCA plot based on the distribution of hard coral and milleporid species at both sites. PC1 accounted for 53.8% of the variation and PC2 accounted for 30.7% of the variation. T, Tómbolo transects; M, Machuca transects.

three of them (*A. palmata*, *P. strigosa*, and *P. clivosa*). In contrast, the coral community at Machuca, while only covering less than 2%, was dominated by the few colonies of *S. radians, S. siderea, P. astreoides,* and *P. porites.*

Raw linear distance measured from the river outlet to the center of each reef correlated positively with percent of hard corals, gorgonians, sponges, zoanthids, and coralline algae (**Table 2**). In contrast, percent cover of macroalgae and seagrasses were negatively correlated with distance from the river outlet. The category of sand, pavement and rubble (SPR) showed a very weak negative correlation as this is one of the dominant categories at both study sites.

DISCUSSION

The coastal reefs near the outlet of the RGM watershed are formed on top of an eolianite-beach rock base and can only be reached through beach access due to rough surf and intense wave action during most of the year. The majority of the coral reef formations in this area lie <3 m depth and due to the prevailing high wave conditions, diving operations can typically only be safely conducted during the months of May–June when winds and wave heights are at their minimum. The Tómbolo Reef site is an area protected by beach rock formations that form a semi-enclosed small bay. This protection may have been a key factor

TABLE 2 | Pearson's correlation coefficients for major benthic categories in regards to distance to the river outlet.

	Distance	C	MA	SPR	GRASS	G	S	Z	CA
Distance	1								
C	0.83071	1							
MA	−0.66543	−0.5635	1						
SPR	−0.07534	−0.40738	−0.46279	1					
GRASS	−0.67646	−0.56989	0.08698	0.25165	1				
G	0.31721	0.20518	−0.15386	−0.15417	−0.22078	1			
S	0.66018	0.51189	−0.45698	−0.06388	−0.35425	0.04812	1		
Z	0.46761	0.35753	−0.27277	−0.13142	−0.31989	0.33106	0.34264	1	1
CA	0.44668	0.50288	−0.33719	−0.18235	−0.31018	0.08308	0.37354	0.13993	1

during the original formation of the reef as waves are somewhat dissipated by this natural barrier. The Scleractinian framework here is dominated by only a small number of coral species. There is a predominance of *A. palmata* and brain corals (*P. clivosa* and *P. strigosa*) with intermingled colonies of *Porites astreoides* and *P. porites* as well as fire corals (*Millepora alcicornis*). Most of the *P. clivosa* colonies are flattened against the hard bottom. A visual inspection performed in 2018 found the branches of some *A. palmata* colonies broken most likely as a consequence of the heavy wave action experienced during the passages of Hurricanes Irma and María in September 2017. The broken branches showed evidence of a thin turf algae layer growing on the scars.

Factors that affect the delivery of terrestrial sediments and other land-based sources of pollution to coral reefs from the river mouth include tides, waves, wind, land orientation, and distance from terrestrial inputs (Woolfe and Larcombe, 1998). In many cases, it is not necessarily the sediment plume itself but rather the continual reworking of the sediment delivered by the plume, that has an impact on the marine ecosystems (Storlazzi et al., 2009). Terrigenous contaminants pose a major threat to coral growth, reproduction and post-disturbance recovery (Wolanski et al., 2004; Fabricius, 2005), and depending on ocean hydrodynamics, can persist and undergo periodic resuspension on reefs for many years (Tribble et al., 2015; Teneva et al., 2016). The Machuca site is located halfway between the RGM outlet and the Tómbolo site. Its proximity to the RGM outlet and lack of physical barriers between them contributes to the direct impact of river plumes throughout the year and even during months with low daily streamflow rates. A possible impact of the river plume is evidenced at Machuca Reef as it shows a substrate of dead hard corals covered by macroalgae, mostly turf and *Dictyota* sp., which differs significantly from the extensive cover of living hard corals at Tómbolo. These formations are heavily eroded and serve as refugia for invertebrate species such as echinoids and asterids. The results described here (i.e., negative correlation in macroalgal cover and positive correlation in percent of Scleractinians with distance from river) are similar to those of Van Woesik et al. (1999) who reported a gradient of terrestrial influence away from the mouths of two rivers in Australia and associated this with recent loss of reef-building capacity on those reefs located nearest to the river mouth.

Hernández et al. (2020) found mean values of 0.07 m^{-1} for Kd_{490} and 0.55 $\mu\text{g l}^{-1}$ for Chl-a for the surrounding waters of PR from 2012 to 2017 in both inner shelf and outer shelf virtual stations. In addition, the researchers highlighted various indicator values for degraded water quality conditions and suggested that for PR these are in the vicinity of $\sim$0.1 m^{-1} for Kd_{490} and $\sim$0.45 $\mu\text{g l}^{-1}$ for Chl-a. Most of our nearshore virtual stations consistently exceeded 0.45 $\mu\text{g l}^{-1}$. In the case of Kd_{490}, stations just north of the river outlet and just north of Machuca Reef (N5–N7) show values that were persistently 2–3 times (with up to 10X higher during the peak Fall rainy season) the proposed indicator value (Hernández et al., 2020). Kd_{490} values at the closest virtual station from Machuca Reef (N5) exceeded the 0.07 m^{-1} mean 66% of any given year compared to that closer to Tómbolo Reef (N4; 33%). For Chl-a, these same stations showed on average 3X the 0.45 $\mu\text{g l}^{-1}$ value and these persisted throughout the study period (**Figure 3**). Chl-a values exceeded the 0.55 $\mu\text{g l}^{-1}$ mean 100% of the year near Machuca Reef and 50% of the year near Tómbolo Reef. These results suggest chronically impaired water quality, particularly at Machuca Reef. Recently, Tuttle and Donahue (2020) proposed a series of thresholds for sediment stress on corals for Hawaiian coral species but that could also be applicable to other regions around the world. While remotely sensed data for suspended sediment analysis is still limited, detailed *in situ* suspended and deposited sediment analyses should be considered for future work on our study sites or elsewhere in PR.

A significant portion of the RGM watershed has been dedicated to cattle farms. Cattle grazing has been known to cause soil erosion and increase in the sediment and particulates delivery in other settings (Brodie et al., 2010). For example, McKergrow et al. (2005) and Mitchell et al. (2005) showed a direct relationship between these land uses and increased sediment and particulates to the Great Barrier Reef in Australia particularly during periods of high river flow associated with monsoonal rainfall events. In addition, in regards to our study sites, the upper portions of the RGM are used for coffee farming, a land use locally known for its ability to increase both surface erosion and mass wasting (Ramos-Scharrón and Figueroa-Sánchez, 2017; Ramos-Scharrón et al., 2021).

Coral species differ in sediment tolerance, light requirements, and salinity preferences and therefore, react differently to sediment exposure (Erftemeijer et al., 2012). Coral traits that affect sediment rejection include colony shape and orientation, calyx size, polyp extensibility, and symbiont preference

(Todd, 2008; Innis et al., 2018). A study by Heery et al. (2018) in Asia showed that reefs located closer to the cities harbor a higher abundance of encrusting or sub-massive species and fewer branching species, leading to a loss in habitat complexity and less invertebrate and fish taxa associated with these reefs. Likewise, in the United States Virgin Islands (USVI), studies have shown a dominance of "weedy" species like *Porites astreoides* and *Siderastrea siderea*, and decreased habitat complexity near developed watersheds (Shaish et al., 2010; Ennis et al., 2016; Oliver et al., 2018). While our study sites are not necessarily located at different distances from major cities, the distance from the river outlet to the Tómbolo Reef is twice that of Machuca Reef. Furthermore, as shown in **Figure 6B** above, our results concur with the mentioned studies from the USVI as *S. siderea* and *P. astreoides* are two of the three dominant species of hard corals on Machuca Reef.

The relatively low diversity of Scleractinian species at Tómbolo Reef, as evidenced by both, the Shannon-Weaver and Simpsons Indexes, may be due to a self-maintained pool of larvae and recruits within this semi-enclosed bay. A genetic analysis of the species composition in this reef is proposed to further confirm this hypothesis. Independently, the high dominance of Scleractinian species, including the threatened *A. palmata* and *Pseudodiploria* sp. at Tómbolo Reef puts it in an honored position as one of the few coral reefs around PR that still shows such high coral cover and one that deserves special attention by the federal and local governmental agencies. Further, its protection may serve as an example for other similar reef areas in PR and the rest of the Caribbean.

DATA AVAILABILITY STATEMENT

The raw data supporting the conclusions of this article will be made available by the authors, without undue reservation.

AUTHOR CONTRIBUTIONS

JT-P was the Science PI and MB-O was the PI of the HICE-PR project. JT-P and LG conducted the reef characterization field work and analysis. CR-S and JO-Z were in charge of the river streamflow and rainfall data analysis. WH and RA conducted the remote sensing water quality analysis. MB-O was in charge of the wave regime analysis. MB-O and RV were the principal investigators of the two projects funded by NASA and NOAA, respectively, and contributed to field activities and data analysis. All authors contributed to the writing of the manuscript.

FUNDING

This research was conducted under the Human Impacts to Coastal Ecosystems (HICE-PR) project funded by the NASA ROSES12 Interdisciplinary Research in Earth Sciences (Grant #: NNX14AJ23G). Part of this research was also conducted under the "Benthic community structure characterization and assessment of turbidity impacts of the north (Manatí and Vega Baja) and south (Guánica) coastal, Puerto Rico" funded by the NOAA Coral Reef Conservation Program (NA17NOS4820079) to Protectores de Cuencas Inc. The participation of WH and RA were in part supported by the National Oceanic and Atmospheric Administration – Cooperative Science Center for Earth System Sciences and Remote Sensing Technologies (NOAA-CESSRST) under the Cooperative Agreement Grant #: NA16SEC4810008. Funds to cover for publication charges were provided by the NASA Ocean Biology and Biogeochemistry Program (Laura Lorenzoni, Program Scientist).

ACKNOWLEDGMENTS

We are extremely thankful to all the students and research assistants from the University of Puerto Rico (UPR) who helped during multiple phases of data collection. Anabella Zuluaga-Montero helped with the CPCe phototransects analysis. Ms. Nahir Cabrera produced the maps used in **Figure 1** of this manuscript. We are thankful to Marianne Cartagena-Colón for helping with aspects of the statistical analysis. We would like to acknowledge the NOAA/NESDIS/STAR Ocean Color and Coral Reef Watch Team (especially Erick Geiger) for providing access and support for the VIIRS satellite imagery. Very special thanks to Para La Naturaleza for aiding with logistics and facilitating the access to the study sites. The content of this manuscript was greatly improved by the contributions of two reviewers. The statements contained within the manuscript/research article are not the opinions of the funding agency or the United States government but reflect the author's opinions.

SUPPLEMENTARY MATERIAL

The Supplementary Material for this article can be found online at: https://www.frontiersin.org/articles/10.3389/fmars.2021.720712/full#supplementary-material

REFERENCES

79 FR §53852 (2014). Endangered and threatened wildlife and plants: Final listing determinations on proposal to list 66 reef-building coral species and to reclassify elkhorn and staghorn corals. NOAA-NMFS. Available online at: https://www.federalregister.gov/documents/2014/09/10/2014-20814/endangered-and-threatened-wildlife-and-plants-final-listing-determinations-on-proposal-to-list-66 (Accessed: March 23, 2021).

Acevedo, R., and Morelock, J. (1989). Modification of coral reef zonation by terrigenous sediment stress. *Palaios* 4, 92–100. doi: 10.2307/3514736

Ángeles, M. E., González, J. E., Ramírez-Beltrán, N. D., Tepley, C. A., and Comarazamy, D. E. (2010). Origins of the Caribbean rainfall bimodal behavior. *J. Geophys. Res.* 115:D11106. doi: 10.1029/2009JD012990

Ballantine, D. L., Appeldoorn, R. S., Yoshioka, P., Weil, E., Armstrong, R., García, J. R., et al. (2008). "Biology and ecology of Puerto Rican coral reefs," in *Coral Reefs of the World, Volume 1 – Coral Reefs of the USA*, eds B. M. Riegl and R. E. Dodge (Dordrecht: Springer Science), 375–406. doi: 10.1007/978-1-4020-6847-8_9

Barreto, M. (1997). *Shoreline Changes at Puerto Rico*. dissertation thesis, Mayaguez PR: University of Puerto Rico, Mayagüez Campus.

Barreto-Orta, M., Méndez-Tejeda, R., Rodríguez, E., Cabrera, N., Díaz, E., and Pérez, K. (2019). State of beaches in Puerto Rico after Hurricane Maria (2017). *Shore Beach* 87, 16–23.

Birkeland, C. (1997). *Life and death of coral reefs*. New York, NY: Chapman and Hall.

Bonkosky, M., Hernández-Delgado, E. A., Sandoz, B., Robledo, I. E., Norat-Ramírez, and Mattei, H. (2009). Detection of spatial fluctuations of non-point source fecal pollution in coral reef surrounding waters in southwestern Puerto Rico using PCR-based assays. *Mar. Poll. Bull.* 58, 45–54. doi: 10.1016/j.marpolbul.2008.09.008

Brodie, J., Schroeder, T., Rohde, K., Faithful, J., Masters, B., Dekker, A., et al. (2010). Dispersal of suspended sediments and nutrients in the Great Barrier Reef lagoon during river-discharge events: conclusions from satellite remote sensing and concurrent flood-plume sampling. *Mar. Freshwater Res.* 61, 651–664. doi: 10.1071/mf08030

Bush, D. M., Webb, R. M. T., González-Liboy, J., and Neal, W. J. (1995). *Living with the Puerto Rico Shore*. North Carolina: Duke University Press.

Cardona-Maldonado, M. (2008). *Assessment of coral reef community structure using water optical properties*. master's thesis, Mayaguez PR: University of Puerto Rico, Mayagüez Campus.

Carlson, R. R., Foo, S. A., and Asner, G. P. (2019). Land use impacts on coral ref health: A ridge-to-reef perspective. *Front. Mar. Sci.* 6:562. doi: 10.3389/fmars.2019.00562

Clark, J. J., and Wilcock, P. R. (2000). Effects of land-use change on channel morphology in northeastern Puerto Rico. *GSA Bull.* 112, 1763–1777. doi: 10.1130/0016-7606(2000)112<1763:eoluco>2.0.co;2

Colin, P. L. (1978). *Marine invertebrates and plants of the living reef*. New Jersey: TFH Publications, Inc.

Commonwealth of Puerto Rico and NOAA (2010). *Puerto Rico's Coral Reef Management Priorities*. Silver Springs: NOAA.

Cramer, K. L., O'Dea, A., Leonard-Pingel, J. S., and Norris, R. D. (2020). Millennial-scale change in the structure of a Caribbean reef ecosystem and the role of human and natural disturbance. *Ecogeography* 43, 283–293. doi: 10.1111/ecog.04722

Cróquer, A., and Weil, E. (2009). Changes in Caribbean coral disease prevalence after the 2005 bleaching event. *Dis. Aquat. Org.* 87, 33–43. doi: 10.3354/dao02164

Daly, C., Helmer, E. H., and Quiñones, M. (2003). Mapping the climate of Puerto Rico, Vieques and Culebra. *Int. J. Climatol.* 23, 1359–1381. doi: 10.1002/joc.937

Doron, M., Babin, M., Mangin, A., and Hembise, O. (2007). Estimation of light penetration, and horizontal and vertical visibility in oceanic and coastal waters from surface reflectance. *J. Geophys. Res.* 112:C06003. doi: 10.1029/2006JC004007

Ennis, R. S., Brandt, M. E., Wilson Grimes, K. L., and Smith, T. B. (2016). Coral reef health response to chronic and acute changes in water quality in St. Thomas, United States Virgin Islands. *Mar. Poll. Bull.* 111, 418–427. doi: 10.1016/j.marpolbul.2016.07.033

Erftemeijer, P. L. A., Riegl, B., Hoeksema, B. W., and Todd, P. A. (2012). Environmental impacts of dredging and other sediment disturbances on corals: a review. *Mar. Poll. Bull.* 64, 1737–1765. doi: 10.1016/j.marpolbul.2012.05.008

Fabricius, K. E. (2005). Effects of terrestrial runoff on the ecology of corals and coral reefs: review and synthesis. *Mar. Poll. Bull.* 50, 125–146. doi: 10.1016/j.marpolbul.2004.11.028

Fabricius, K. E., and Wolanski, E. C. (2000). Rapid smothering of coral reef organisms by muddy marine snow. *Estuar. Coast. Shelf Sci.* 50, 115–120. doi: 10.1006/ecss.1999.0538

García-Sais, J., Appeldoorn, R., Battista, T., Bauer, L., Bruckner, A., Caldow, C., et al. (2008). *The state of coral reef ecosystems of Puerto Rico The state of coral reef ecosystems of the United States and Pacific Freely Associated States*. Washington, DC: Kindle direct publishing, 75–116.

Gellis, A. C. (2012). Factors influencing storm-generated suspended-sediment concentrations and loads in four basins of contrasting land use, humid-tropical Puerto Rico. *Catena* 104, 39–57. doi: 10.1016/j.catena.2012.10.018

Goenaga, C., and Cintrón, G. (1979). *Inventory of the Puerto Rican Coral Reefs. Report to the Department of Natural and Environmental Resources of the Commonwealth of Puerto Rico*. San Juan, PR: DNER.

Golbuu, Y., Fabricius, K., Victor, S., and Richmond, R. H. (2008). Gradients in coral reef communities exposed to muddy river discharge in Pohnpei, Micronesia. *Est. Coast. Shelf Sci.* 76, 14–20. doi: 10.1016/j.ecss.2007.06.005

Grau, R. H., Aide, T. M., Zimmerman, J. K., Thomlinson, J. R., Helmer, E., and Zou, X. (2003). The ecological consequences of socioeconomic and land-use changes in postagriculture Puerto Rico. *BioScience* 53, 1159–1168. doi: 10.1641/0006-3568(2003)053[1159:tecosa]2.0.co;2

Harvell, D., Jordán-Dahlgren, E., Merkel, E., Rosenberg, E., Raymundo, L., Smith, G., et al. (2007). Coral disease, environmental drivers, and the balance between coral and microbial associates. *Oceanography* 20, 172–195. doi: 10.5670/oceanog.2007.91

Heery, E. C., Hoeksema, B. W., Browne, N. K., Reimer, J. D., Ang, P. O., Huang, D., et al. (2018). Urban coral reefs: degradation and resilience of hard coral assemblages in coastal cities of East and Southeast Asia. *Mar. Poll. Bull.* 135, 654–681. doi: 10.1016/j.marpolbul.2018.07.041

Helmer, E. H., Brandeis, T. J., Lugo, A. E., and Kennaway, T. (2008). Factors influencing spatial pattern in tropical forest clearance and stand age: Implications for carbon storage and species diversity. *J. Geophys. Res.* 113:G02S04. doi: 10.1029/2007/G000568

Hernández, W. J., Ortiz-Rosa, S., Armstrong, R. A., Geiger, E. F., Eakin, C. M., and Warner, R. A. (2020). Quantifying the Effects of Hurricanes Irma and Maria on Coastal Water Quality in Puerto Rico using Moderate Resolution Satellite Sensors. *Remote Sens.* 12:964. doi: 10.3390/rs12060964

Hernández Delgado, E. A., Medina-Muñiz, J. L., Mattei, H., and Norat-Ramírez, J. (2017). Unsustainable land use, sediment-laden runoff, and chronic raw sewage offset the benefits of coral reef ecosystems in a no-take marine protected area. *Env. Mgmt. Sust. Dev.* 6, 292–333. doi: 10.5296/emsd.v6i2.10687

Hernández-Delgado, E. A., Sandoz, B., Bonkosky, M., Norat-Ramírez, J., and Mattei, H. (2008). "Impacts of non-point source sewage pollution on Elkhorn coral, *Acropora palmata* (Lamarck) assemblages of the southwestern Puerto Rico shelf," in *Proceedings of the 11th Int. Coral Reef Symp*, (Lauderdale),

Hughes, T. P., Barnes, M. L., Bellwood, D. R., Cinner, J. E., Cumming, G. S., Jackson, J. B., et al. (2017). Coral reefs in the Anthropocene. *Nature* 546, 82–90.

Humann, P., and DeLoach, N. (2013). *Reef coral identification: Florida, Caribbean, Bahamas*. Jacksonville, FL: New World Publications, Inc.

Innis, T., Cunning, R., Wall, C. B., and Gates, R. D. (2018). Coral color and depth drive symbiosis ecology of *Montipora capitata* in Kane'ohe Bay, O'ahu, Hawai'i. *Coral Reefs* 37, 423–430. doi: 10.1007/s00338-018-1667-0

Kohler, K. E., and Gill, S. M. (2006). Coral Point Count with Excel extensions (CPCe): a visual basic program for the determination of coral and substrate coverage using random point count methodology. *Comp. Geosci.* 32, 1259–1269. doi: 10.1016/j.cageo.2005.11.009

Kroon, F. J., Thorburn, P., Schaffelke, B., and Whitten, S. (2016). Towards protecting the Great Barrier Reef from land-based pollution. *Glob. Change Biol.* 22, 1985–2002. doi: 10.1111/gcb.13262

Larsen, M. C. (2012). "Landslides and sediment budgets in four watersheds in eastern Puerto Rico," in *Water quality and landscape processes of four watersheds in eastern Puerto Rico*, eds S. F. Murphy and R. F. Stallard (Washington, D.C: U.S. Geological Survey Professional Paper), 153–178. doi: 10.3133/pp1789f

Larsen, M. C., and Santiago Román, A. (2001). "Mass wasting and sediment storage in a small montane watershed: an extreme case of anthropogenic disturbance in the humid tropics," in *Geomorphic Processes and Riverine Habitat, Water Science, and Application*, Vol. 4, eds J. M. Dorava, F. Fitzpatrick, B. B. Palcsak, and D. R. Montgomery (American Geophysical Union Monograph*), 119–138. doi: 10.1029/ws004p0119

Larsen, M. C., and Webb, R. M. T. (2009). Potential effects of runoff, fluvial sediment, and nutrient discharges on the coral reefs of Puerto Rico. *J. Coastal Res.* 25, 189–208. doi: 10.2112/07-0920.1

Littler, D. S., and Littler, M. M. (2000). *Caribbean reef plants: An identification guide to the reef plants of the Caribbean, Bahamas, Florida and Gulf of Mexico*. Washington DC: OffShore Graphics, Inc.

López, T., Aide, T. M., and Scatena, F. N. (1998). The effect of land use on soil erosion in the Guadiana Watershed in Puerto Rico. *Carib. J. Sci.* 34, 298–307.

McKergrow, L. A., Prosser, I. P., Hughes, A. O., and Brodie, J. (2005). Regional scale nutrient modelling: exports to the Great Barrier Reef World Heritage Area. *Mar. Poll. Bull.* 51, 186–199. doi: 10.1016/j.marpolbul.2004.11.030

McLaughlin, C. J., Smith, C. A., Buddemeier, R. W., Bartley, J. D., and Maxwell, B. A. (2003). Rivers, runoff, and reefs. *Glob. Planet. Change* 39, 191–199. doi: 10.1016/s0921-8181(03)00024-9

Mikelsons, K., and Wang, M. (2019). Optimal satellite orbit configuration for global ocean color product coverage. *Opt. Express* 27, A445–A457.

Mitchell, C., Brodie, J., and White, I. (2005). Sediments, nutrients, and pesticide residues in event flow conditions in streams of the Mackay Whitsunday Region, Australia. *Mar. Poll. Bull.* 51, 23–36. doi: 10.1016/j.marpolbul.2004.10.036

Monroe, W. H. (1980). *Some tropical landforms of Puerto Rico*, Vol. 1159. Washington, D.C: Geological Survey Professional Paper, 39.

Morelock, J., and Barreto, M. (2003). An update of coastal erosion in Puerto Rico. *Shore Beach* 71, 7–12.

Morelock, J., Capella, J., García, J. R., and Barreto, M. (2000). "Puerto Rico - Seas at the Millennium," in *Seas at the Millennium*, ed. C. R. C. Sheppard (London: Oxford Press).

Morelock, J., Ramirez, W., and Barreto, M. (2010). *Puerto Rico. Encyclopedia of World's coastal landforms*. Australia: Pergamum Press, 289–294.

Morelock, J., Schwartz, M. L., Hernández-Avila, M., and Hatfield, D. M. (1985). Net shore-drift on the north coast of Puerto Rico. *Shore Beach* 53, 16–21.

Norat-Ramírez, J., Méndez-Lázaro, P., Hernández-Delgado, E. A., Mattei-Torres, H., and Cordero-Rivera, L. (2019). A septic waste index model to measure impact of septic tanks on coastal water quality and coral reef communities in Rincón, Puerto Rico. *Ocean Coast. Manag.* 169, 201–213. doi: 10.1016/j.ocecoaman.2018.12.016

Norström, A. V., Nyström, M., Jouffray, J. B., Folke, C., Graham, N. A. J., Moberg, F., et al. (2016). Guiding coral reef futures in the Anthropocene. *Front. Ecol. Env.* 1499:490–498. doi: 10.1002/fee.1427

Oliver, L. M., Fisher, S. W., Fore, L., Smith, A., and Bradley, P. (2018). Assessing land use, sedimentation, and water quality stressors as predictors of coral reef condition in St. Thomas, U.S. Virgin Islands. *Environ. Monitor. Assess.* 190, 1–16.

Otaño-Cruz, A., Montañez-Acuña, A. A., García-Rodríguez, N. M., Díaz-Morales, D. M., Benson, E., Cuevas, E., et al. (2019). Caribbean near-shore coral reef benthic community response to changes in sedimentation dynamics and environmental conditions. *Front. Mar. Sci.* 6:551.

Otaño-Cruz, A., Montañez-Acuña, A. A., Torres-López, V., Hernández-Figueroa, E. M., and Hernández-Delgado, E. A. (2017). Effects of changing weather, oceanographic conditions, and land-uses on spatio-temporal variation of sedimentation dynamics along near-shore coral reefs. *Front. Mar. Sci.* 4:249.

Ott, R. L. (1993). *An introduction to statistical methods and data analysis*. California: Duxbury Press.

Philipp, E., and Fabricius, K. (2003). Photophysiological stress in scleractinian corals in response to short-term sedimentation. *J. Exp. Mar. Biol. Ecol.* 287, 57–78. doi: 10.1016/50022-0981(02)00495-1

Pinto, P., Cabral, P., Caetano, M., and Alves, M. F. (2009). Urban growth on coastal erosion vulnerable stretches. *J. Coastal Res.* 56, 1567–1571.

Putnam, H. M., Barott, K. L., Ainsworth, T. D., and Gates, R. D. (2017). The vulnerability and resilience of reef-building corals. *Curr. Biol.* 27, R528–R540. doi: 10.1016/j.cub.2017.04.047

Ramos-Scharrón, C. E., Arima, E. Y., Guidry, A., Ruffe, D., and Vest, B. (2021). Sediment mobilization by hurricane-driven shallow landsliding in a wet subtropical watershed. *J. Geophys. Res. Earth Surf.* 126:e2020JF006054.

Ramos-Scharrón, C. E., and Figueroa-Sánchez, Y. (2017). Plot-, farm-, and watershed-scale effects of coffee cultivation in runoff and sediment production in western Puerto Rico. *J. Environ. Manag.* 202, 126–136. doi: 10.1016/j.jenvman.2017.07.020

Ramos-Scharrón, C. E., and Thomaz, E. L. (2016). Runoff development and soil erosion in a wet tropical montane setting under coffee cultivation. *Land Degr. Dev.* 28, 936–945. doi: 10.1002/ldr.2567

Ramos-Scharrón, C. E., Torres-Pulliza, D., and Hernández-Delgado, E. A. (2015). Watershed- and island wide-scale land cover changes (1930s-2004) and their potential effects on coral reef systems. *Sci. Total Env.* 506-507, 241–251. doi: 10.1016/j.scitotenv.2014.11.016

Reyer, C. P., Adams, S., Albrecht, T., Baarsch, F., Boit, A., Trujillo, N. C., et al. (2017). Climate change impacts in Latin America and the Caribbean and their implications for development. *Reg.Env. Chang.* 17, 1601–1621. doi: 10.1007/s10113-015-0854-6

Rogers, C. S. (1990). Responses of coral reefs and reef organisms to sedimentation. *Mar. Ecol. Progr. Ser.* 62, 185–202. doi: 10.3354/meps062185

Rudel, T. K., Pérez-Lugo, M., and Zichal, H. (2010). When fields revert to forest: development and spontaneous reforestation in post-war Puerto Rico. *Prof. Geogr.* 52, 386–397. doi: 10.1111/0033-0124.00233

Ryan, K. E., Walsh, J. P., Corbett, D. R., and Winter, A. (2008). A record of recent change in terrestrial sedimentation in a coral-reef environment, La Parguera, Puerto Rico: a response to coastal development? *Mar. Poll. Bull.* 56, 1177–1183. doi: 10.1016/j.marpolbul.2008.02.017

Shaish, L., Levy, G., Katzir, G., and Rinkevich, B. (2010). Employing a highly fragmented, weedy coral species in reef restoration. *Ecol. Eng.* 36, 1424–1432. doi: 10.1016/j.ecoleng.2010.06.022

Storlazzi, C. D., Field, M. E., Bothner, M. H., Presto, M. K., and Draut, A. E. (2009). Sedimentation processes in a coral reef embayment: Hanalei Bay. *Kauai. Mar. Geol.* 264, 140–151. doi: 10.1016/j.margeo.2009.05.002

Storlazzi, C. D., Norris, B. K., and Rosenberger, K. J. (2015). The influence of grain size, grain color, and suspended-sediment concentration on light attenuation: why fine-grained terrestrial sediment is bad for coral reef ecosystems. *Coral Reefs* 34, 967–975. doi: 10.1007/s00338-015-1268-0

Teneva, L. T., McManus, M. A., Jerolmon, C., Neuheimer, A. B., Clark, S. J., Walker, G., et al. (2016). Understanding reef flat sediment regimes and hydrodynamics can inform erosion mitigation on land. *Collabra* 2, 1–12.

Todd, P. A. (2008). Morphological plasticity in scleractinian corals. *Biol. Rev.* 83, 315–337. doi: 10.1111/j.1469-185x.2008.00045.x

Torres, J. L. (2001). Impacts of sedimentation on the growth rates of *Montastraea annularis* in southwest. *Puerto Rico. Bull. Mar. Sci.* 69, 631–637.

Torres, J. L., and Morelock, J. (2002). Effects of terrigenous sediments influx on the coral cover and linear extension rates of three Caribbean massive coral species. *Carib. J. Sci.* 38, 222–229.

Tribble, G., Stock, J., and Jacob, J. (2015). "Watershed processes from ridge to reef: consequences of feral ungulates for coral reef and effects of watershed management," in *Proc. 5th Interagency Conf. on Research in Watersheds and Headwaters to Estuaries: Advances in Watershed Science and Management*, ed. S. E. Christina (Asheville, NC: US Department of Agriculture, US Forest Service), 194.

Tuttle, L. J., and Donahue, M. J. (2020). *Thresholds for sediment stress on corals: a systematic review and meta-analysis*. Honolulu, HI: NOAA Fisheries Pacific Islands, Habitat Conservation Division, 75.

Tuttle, L. J., Johnson, C., Kolinski, S., Minton, D., and Donahue, M. J. (2020). How does sediment exposure affect corals? A systematic review protocol. *Environ. Evid.* 9:17. doi: 10.1186/s13750-020-00200-0

Van Woesik, R., Tomascik, T., and Blake, S. (1999). Coral assemblages and physico-chemical characteristics of the Whitsunday Islands: evidence of recent community changes. *Mar. Freshwater Res.* 50, 427–440. doi: 10.1071/mf97046

Veron, J. E. N. (1995). *Corals in space and time*. Sydney: UNSW Press.

Veron, J. E. N., Stafford-Smith, M. G., Turak, E., and DeVantier, L. M. (2016). *Corals of the World*. Available online at: http://coralsoftheworld.org (Accessed: 15 January 2021).

Wakwella, A., Mumby, P. J., and Roff, G. (2020). Sedimentation and overfishing drive changes in early succession and coral recruitment. *Proc. Royal Soc. B.* 287:20202575. doi: 10.1098/rspb.2020.2575

Wang, M., and Son, S. (2016). VIIRS-derived chlorophyll-a using the ocean color index method. *Remote Sens. Env.* 182, 141–149. doi: 10.1016/j.rse.2016.05.001

Wang, M., Son, S., and Harding, L. W. Jr. (2009). Retrieval of diffuse attenuation coefficient in the Chesapeake Bay and turbid ocean regions for satellite ocean color applications. *J. Geophys. Res: Oceans.* 114:C10011. doi: 10.1029/2009JC005286

Wolanski, E., Richmond, R. H., and McCook, L. (2004). A model of the effects of land-based, human activities on the health of coral reefs in the Great Barrier Reef and in Fouha Bay. Guam, Micronesia. *J. Mar. Syst.* 46, 133–144. doi: 10.1016/j.jmarsys.2003.11.018

Woolfe, K. J., and Larcombe, P. (1998). Terrigenous sediment accumulation as a regional control on the distribution of reef carbonates. *Special Public. Internat. Assoc. Sediment.* 25, 295–310. doi: 10.1002/9781444304879.ch16

Wusinich-Méndez, D., López-Rivera, M., and Díaz, E. (2007). "Puerto Rico Coral Reef MPA Summary," in *Report on the Status of Marine Protected Areas in Coral Reef Ecosystems of the United States Volume 1: Marine Protected Areas Managed by U.S. States, Territories, and Commonwealths: 2007. NOAA Technical Memorandum CRCP 2*, eds D. Wusinich-Méndez and C. Trappe (Silver Spring MD: NOAA Coral Reef Conservation Program), 103–116.

Zuluaga-Montero, A. (2003). *Fish and epibenthic community structure in eight reefs with contrasting environmental conditions*. dissertation thesis, San Juan PR: University of Puerto Rico, Rio Piedras Campus.

Conflict of Interest: The authors declare that the research was conducted in the absence of any commercial or financial relationships that could be construed as a potential conflict of interest.